Journal of the Indian Chemical Society 100 (2023) 100981

Contents lists available at ScienceDirect

Journal of the Indian Chemical Society

journal homepage: www.journals.elsevier.com/journal-of-the-indian-chemical-society

Molecular docking, HOMO-LUMO and quantum chemical computation analysis of anti-glyoximehydrazone derivatives containing pyrazolone moiety and their transition metal complexes

Nursabah Sarikavakli [a,*], Onur Genç [b], Şerife Gökçe Çalişkan [b], Fatma Erol [c]

[a] Department of Chemistry, Faculty of Sciences, Aydin Adnan Menderes University, 09010, Aydin, Turkey
[b] Department of Physics, Faculty of Sciences, Aydin Adnan Menderes University, 09010, Aydin, Turkey
[c] Technical Sciences Vocational School, Gazi University, Ostim, Ankara, 06374, Turkey

ARTICLE INFO

Keywords:
Hydrazones
Pyrazolones
Transition metal complexes
HOMO-LUMO analysis
Molecular docking

ABSTRACT

In this study, in order to obtain biologically active compounds, a series of anti-glyoximehydrazone ligands bearing vic-dioxime, hydrazone, and pyrazole moieties and their (O•••H–O) bridged nickel(II), cobalt(II) and copper(II) metal complexes were prepared. Further, the molecular docking studies were carried out on those ligands and their nickel(II), cobalt(II) and copper(II) metal complexes to analyze the interaction with EGFR Kinase domain complexed with tak-285 (PDB ID: 3POZ) and human androgen receptor T877A mutant (PDB ID:2OZ7). In addition, the compounds were optimized by using B3LYP/6-311G+(d,p) level of Density Functional Theory (DFT) to evaluate the HOMO–LUMO contours and quantum chemical parameters. Also, bioactivity analysis were performed.

Metal complexes had higher binding affinities against 3POZ and 2OZ7. The most promising compounds for 3POZ were nickel(II) and copper(II) metal complexes. However, for the 2OZ7 target receptor, cobalt(II) and copper(II) metal complexes were the possible hit compounds. Furthermore, cobalt(II) metal complex of ligand two was found to be the most reactive one among others. Moreover, it had the highest ω which is related to a potent higher electrophilic character. It was determined that all the compounds had moderate bioactivity.

In conclusion, nickel(II), cobalt(II), and copper(II) complexes could be powerful hit compounds for anti-cancer drug discovery studies.

1. Introduction

In recent years, theoretical chemistry has gained importance in investigating the structural, physical and biological properties of materials. The results obtained from the theoretical studies help to predict and interpret the results that can be obtained from the experimental studies where obtaining the theoretical results is much cheaper and faster than the experimental results. Therefore, it is very important to make theoretical calculations before the experiments in order to avoid wasting time and money for the experiments [1,2].

Vicinal dioximes are, one of these analogs, used extensively not only for their antitumor activity but also for their biological properties like fungicidal, bactericidal, insecticidal, analgesic, anti-inflammatory, and antioxidant activity [3,4]. These biologically active ligands, including oximes, give rise to more potent compounds when they coordinated with certain transition metals called metal complexes.

The higher stability of the complexes prepared from vicinal dioximes enables researchers to use them as e.g. model compounds for some biological systems [5] or trace metal analysis [6].

The pyrazolone core has many biological activities, including several pharmaceuticals currently on the market. Moreover, pyrazolone derivatives have numerous applications in fluorescent materials, dyes, agrochemicals, and more. Therefore, the interest in pyrazole chemistry is still ongoing [7–12].

For all these reasons, both pyrazolones, oximes and pyrazolone-oxime compounds have become the focus of chemical and pharmaceutical research.

Cancer is one of the most significant health problems at the present

* Corresponding author.
E-mail addresses: nsarikavakli@adu.edu.tr (N. Sarikavakli), onur.genc@adu.edu.tr (O. Genç), gcaliskan@adu.edu.tr (Ş.G. Çalişkan), fnuralin@gazi.edu.tr (F. Erol).

https://doi.org/10.1016/j.jics.2023.100981
Received 27 September 2022; Received in revised form 5 January 2023; Accepted 21 March 2023
Available online 22 March 2023
0019-4522/© 2023 Indian Chemical Society. Published by Elsevier B.V. All rights reserved.

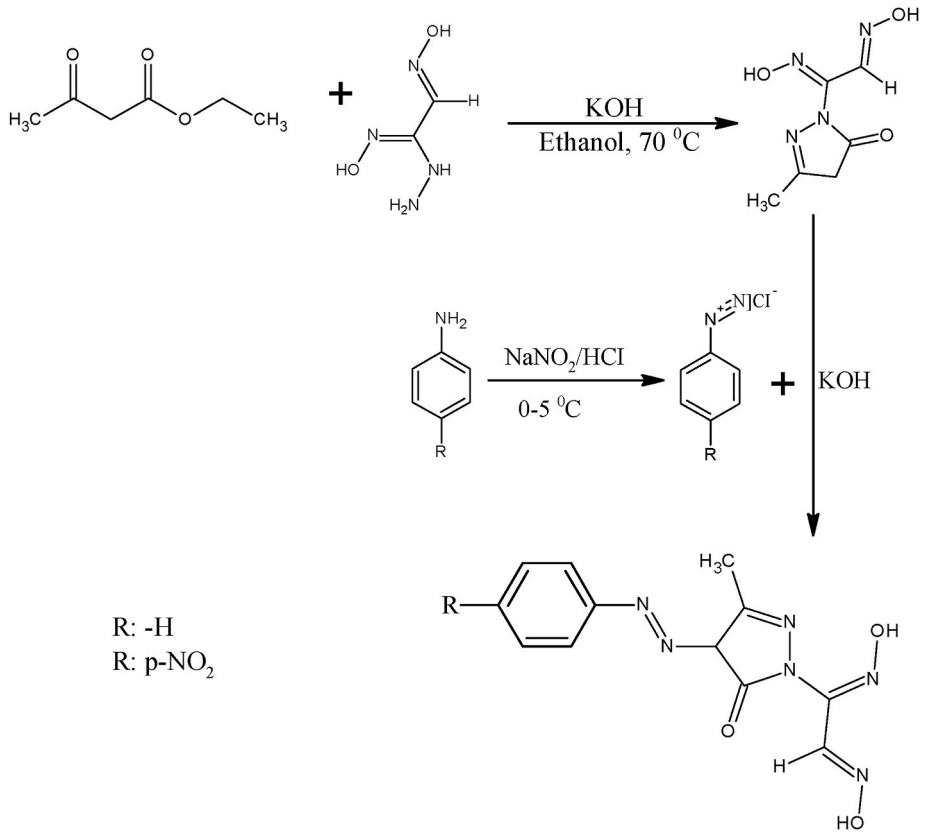

Scheme 1. General route for the synthesis of Pyrazolone-containing anti-glyoximehydrazone ligands $\mathbf{H_2L^1}$ and $\mathbf{H_2L^2}$ [16,17].

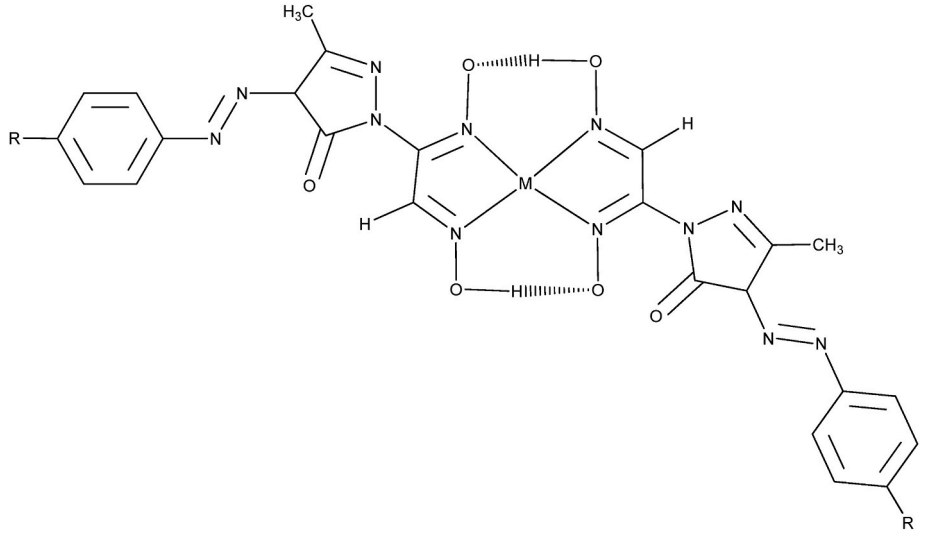

Scheme 2. The general structure of the transition metal complexes of ligands $\mathbf{H_2L^1}$ and $\mathbf{H_2L^2}$. [15,16].

time and for humans the second most mortal disease after cardiovascular diseases. There are various methods such as chemotherapy and radiotherapy used in cancer treatment, and among these, chemotherapy is the most preferred. However, chemotherapy has various side effects such as hair loss, diarrhea and vomiting. Although chemotherapy is effective in cancer treatment, researchers are working to develop new drugs which are target-focused and less toxic due to existing side effects. There are a few studies in which the effects of pyrazolone and its metal complexes on cancer cells were investigated. For instance, Althagafi et al. [13] synthesized pyrazolone derivatives and its Ag(I) complexes and investigated their anti-cancer effects by means of physicochemical, DNA binding, antitumor, and theoretical implementations. Besides, Alhasani et al. [14] evaluated the effects of mono- and bimetallic complexes of pyrazolone-based ligand by characterization, antitumor and molecular docking studies. These researchers reported the positive effects of these compounds however there should be more studies that investigate them from different perspectives.

Considering all the information provided above, we have investigated a series of anti-glyoximehydrazine bearing the pyrazolone group by means of molecular docking, Density Functional Theory (DFT) and in

Table 1
Binding energy values and the interactions between the compounds and target proteins.

Compound	Target Proteins	Binding Energy (kcal/mol)	Residue	Distance (Å)	Interaction Type
H_2L^1	3POZ	−5.9	Asn771	2.940	Conventional hydrogen bond
			Arg776	2.999	Conventional hydrogen bond
			Lys852	2.843	Conventional hydrogen bond
			Val769	2.365	Conventional hydrogen bond
			Asp770	3.885	Pi-Anion
	2OZ7	−5.8	Trp751	3.266	Conventional hydrogen bond
			Ala748	2.705	Conventional hydrogen bond
			Thr755	3.714	Pi-Sigma
			Pro801	4.742	Alkyl
			Leu805	4.272	Alkyl
			Trp751	4.663	Pi-Alkyl
			Trp751	4.978	Pi-Alkyl
			Phe804	4.862	Pi-Alkyl
$Ni(H_2L^1)_2$	3POZ	−9.1	Lys846	3.130	Conventional hydrogen bond
			Lys852	3.164	Conventional hydrogen bond
			Asn771	3.267	Carbon-hydrogen bond
			Asp1014	4.213	Pi-Anion
			Leu703	3.954	Pi-Sigma
			Leu703	3.789	Pi-Sigma
			Pro772	4.057	Alkyl
	2OZ7	−8.7	Phe826	4.569	Pi-pi T-shaped
			Leu830	4.336	Alkyl
			Pro723	4.857	Alkyl
			Phe673	4.588	Pi-Alkyl
			Tyr834	3.887	Pi-Alkyl
			Val676	5.099	Pi-Alkyl
			Pro723	4.122	Pi-Alkyl
$Co(H_2L^1)_2$	3POZ	−8.4	Tyr915	3.261	Conventional hydrogen bond
			Pro934	3.496	Conventional hydrogen bond
			Ser912	3.816	Pi-Donor hydrogen bond
			Arg932	4.627	Pi-Alkyl
			Val948	5.289	Pi-Alkyl
	2OZ7	−8.9	His776	3.091	Conventional hydrogen bond
			His776	2.916	Conventional hydrogen bond
			Gln783	3.354	Conventional hydrogen bond
			His776	4.624	Pi-pi stacked
			Phe876	3.654	Pi-pi stacked
			Phe876	5.304	Pi-Alkyl
			Leu880	5.384	Pi-Alkyl
$Cu(H_2L^1)_2$	3POZ	−9.2	Tyr915	2.993	Conventional hydrogen bond
			Pro834	3.666	Carbon-hydrogen bond
			Lys913	3.597	Carbon-hydrogen bond
			Tyr944	3.484	Pi-Donor hydrogen bond
			Arg932	4.983	Pi-Alkyl
			Val948	5.047	Pi-Alkyl
			Pro934	4.914	Pi-Alkyl
	2OZ7	−8.6	Arg871	3.056	Conventional hydrogen bond
			Arg871	3.123	Conventional hydrogen bond
			Gln875	3.150	Conventional hydrogen bond
			Tyr915	3.294	Pi-Donor hydrogen bond
			Phe878	4.900	Pi-pi T-shaped
			Lys912	4.544	Alkyl
			Pro868	4.883	Pi-Alkyl
			Leu907	4.564	Pi-Alkyl
H_2L^2	3POZ	−6.0	Tyr813	3.304	Conventional hydrogen bond
			Asn816	2.895	Conventional hydrogen bond
			Gln791	3.288	Carbon-hydrogen bond
			His850	5.234	Pi-Pi T-shaped
			Pro772	4.973	Pi-Alkyl
	2OZ7	−6.4	Arg752	3.889	Pi-Cation
			Arg752	4.003	Alkyl
			Trp751	5.311	Pi-Alkyl
			Pro682	5.088	Pi-Alkyl
$Ni(H_2L^2)_2$	3POZ	−8.5	Tyr813	3.304	Conventional hydrogen bond
			Asn816	2.895	Conventional hydrogen bond
	2OZ7	−7.8	Ser782	3.053	Conventional hydrogen bond
			Ser782	3.016	Conventional hydrogen bond
			Gln783	2.777	Conventional hydrogen bond
			Lys883	3.083	Conventional hydrogen bond
			Ser782	3.262	Carbon-hydrogen bond
			Arg786	3.471	Carbon-hydrogen bond
			Phe876	4.111	Pi-pi stacked
$Co(H_2L^2)_2$	3POZ	−8.4	Asn771	3.356	Conventional hydrogen bond
			Asn771	3.101	Conventional hydrogen bond
			Lys846	3.214	Conventional hydrogen bond
			Lys852	3.179	Conventional hydrogen bond
			Arg776	3.425	Carbon-hydrogen bond
			Asp770	3.986	Pi-Anion
			Asp1014	4.090	Pi-Anion
			Pro772	5.413	Pi-Alkyl
	2OZ7	−9.0	Tyr781	3.048	Conventional hydrogen bond
			Ser782	2.939	Conventional hydrogen bond
			Arg871	2.961	Conventional hydrogen bond
			Glu872	4.204	Pi-Anion
			Glu872	3.553	Pi-Sigma
			Phe876	4.102	Pi-pi stacked
$Cu(H_2L^2)_2$	3POZ	−8.5	Lys875	3.178	Conventional hydrogen bond
			Lys879	2.883	Conventional hydrogen bond
			Gly917	3.242	Conventional hydrogen bond
			Gly719	3.528	Carbon-hydrogen bond

(*continued on next page*)

Table 1 (*continued*)

Compound	Target Proteins	Binding Energy (kcal/mol)	Residue	Distance (Å)	Interaction Type
			Asp916	3.589	Carbon-hydrogen bond
			Ala722	4.208	Alkyl
			Pro919	4.824	Pi-Alkyl
			Arg841	5.460	Pi-Alkyl
	2OZ7	−9.4	Tyr739	2.985	Conventional hydrogen bond
			Tyr739	3.180	Conventional hydrogen bond
			Gln902	3.329	Conventional hydrogen bond
			Lys905	2.994	Conventional hydrogen bond
			Val713	3.566	Carbon-hydrogen bond
			Leu821	4.935	Alkyl
			Lys822	4.278	Alkyl
			Met734	4.598	Alkyl
			Pro817	4.611	Pi-Alkyl
			Val716	4.576	Pi-Alkyl

terms of drug-likeness properties.

2. Material and methods

To investigate the visualization of intermolecular interactions of anti-glyoximehydrazone bearing the pyrazolone group, a series of anti-glyoximehydrazone bearing the pyrazolone group phenylamine-anti-glyoximehydrazone, H_2L^1, p-nitrophenylamine-anti-glyoximehydrazone, H_2L^2, and their nickel(II), cobalt(II) and copper(II) metal complexes, that we previously synthesized and characterized their structure Schemes 1 and 2, were studied.

2.1. General procedure for the synthesis of the pyrazolone-containing anti-glyoximehydrazone ligands (H_2L^1 and H_2L^2)

In the first phase of our work, our starting material, anti-glyoximehydrazine,(GH_2), which had been synthesized and gained to the literature by us for the first time in the manner of our previous studies, was synthesized with anti-chlorglyoxime and hydrazine hydrate [15]. Since this parent compound decomposes easily at room temperature it was used as obtained without further purification.

In the second phase of our study, Pyrazolone-containing anti-glyoximehydrazone compounds, which was first synthesized by us, was synthesized by reacting (GH_2), and ethylacetoacetate (EAA) in a mixture of KOH and ethanol at 70 °C. Ethyl acetoacetate (EAA) is added dropwise to the (GH_2), solution with continuous stirring in the presence of KOH and mixed for 60 min. While the solution is mixing, the substance begins to precipitate after a while. The precipitated Pyrazolone-containing anti-glyoximehydrazone ligands H_2L^1 and H_2L^2 compounds (Sheme 1) is filtered, washed several times with with cold distilled water and dried.

2.2. General procedure for the synthesis of the transition metal complexes

For the synthesis of all the three transition metal complexes, a general method was used [6]:

In the final stage of our work, the ligands (H_2L^1 and H_2L^2), were dissolved in absolute ETOH at refluxing temperature. A solution of nickel(II), cobalt(II) and copper(II) metal salts in water was added dropwise into the ligand solution with continuous stirring. A distinct change in color and a decrease in the pH value (~3.0–3.5) of the solution was observed. NaOH (1%) in water was added to adjust the pH ~5–5.5 and the reaction mixture was cooled to room temperature. Mixtures have been stirred by the 1 h at 50 °C on a water bath so as to ensure complete precipitation of complexes. After 1 h the precipitated solid has been filtered, washed by means of hot ETOH also dehydrated in vacuum. Proposed structures for the monomeric $Ni(H_2L^1)_2$, $Co(H_2L^1)_2$, $Cu(H_2L^1)_2$ and $Ni(H_2L^2)_2$, $Co(H_2L^2)_2$, $Cu(H_2L^2)_2$ as well as the pyrazolone-containing glyoxime hydrazone ligands are given in Scheme 2.

2.3. Molecular docking studies

The binding mechanism of the newly synthesized compounds to EGFR Kinase domain complexed with tak-285 (PDB ID: 3POZ) and human androgen receptor T877A mutant (PDB ID: 2OZ7) was investigated via molecular docking method. The X-ray crystallographic structures of the target proteins were downloaded from RSCB protein data bank. Target proteins were prepared for docking by removing water molecules and adding polar hydrogen atoms and also Kollmann charges. For this process, AutoDock tools 1.5.7 software (ADT, The Scripps Research Institute, La Jolla, CA, USA) was used. For the compounds' preparation, 2D structures were drawn by ChemSketch software. Furthermore, 3D structures were generated, optimized with the MM2 force field for achieving the minimum energy value, and converted to PDB format by Avogadro software. By using Autodock Vina [18] the compounds were docked on the EGFR Kinase domain complexed with tak-285 and human androgen receptor T877A mutant target proteins. The visualization of the ligand-protein interaction complex was performed by using DS visualizer Software. Moreover, the molecular docking method was validated by self-docking of the co-crystalized ligands tak-285 (PDB ID:03P) in EGFR Kinase domain complexed with tak-285 and cyproterone acetate (PDB ID:CA4) in human androgen receptor T877A mutant. The co-crystalized ligands were extracted from the protein and re-docked in the same position. The pose with the lowest energy and the initial pose were superimposed and the root mean square deviation (RMSD) was measured. The RMSD value must be smaller than 2 Å for a valid docking procedure [19].Furthermore, the inhibition constant (K_i) was calculated by using the binding energy value obtained by docking procedure. Equation (1) was used for the calculation of K_i value. For being a hit compound K_i value must be small and be in the micromolar range [20].

$$K_i = 10^{(Binding\ Energy \div 1.366)} \quad (1)$$

2.4. Frontier molecular orbitals and quantum chemical calculations

The optimization of the compounds was performed by using Gaussian 09 software [21]. For this process, B3LYP/6-311G+(d,p) level basic set of DFT was used. Afterward, the Frontier Molecular Orbitals (FMO) which were the highest occupied molecular orbital (HOMO) and lowest unoccupied molecular orbital (LUMO) were extracted and the energy gap was calculated by the difference between HOMO and LUMO energy values. Furthermore, quantum chemical parameters were calculated in order to predict the behavior of compounds and to get information about the transition state energies [22].

2.5. Bioactivity analysis

The bioactivity scores of H_2L^1, H_2L^2 and their nickel(II), cobalt(II) and copper(II) complexes were determined by online www.molinspiration.com [23] web site. ChemDraw software was used to obtain the SMILES notations of the compounds. GPCR ligand, ion channel modulator, kinase inhibitor, nuclear receptor ligand, protease inhibitor and enzyme inhibitor parameters were determined by uploading the SMILES notation of the compound to the online software.

3. Result and discussion

In the current study, Pyrazolone-containing anti-glyoximehydrazone ligands H_2L^1, H_2L^2 and their nickel(II), cobalt(II) and copper(II) complexes were obtained in three steps.

In the first step, our starting substance, anti- glyoximehydrazine, GH_2, which was synthesized and brought to the literature by us for the first time in our previous studies, was synthesized in terms of the reaction of anti-chloroglyoxime and hydrazinium hydroxide in an alcohol-water mixture (4:1) [15].

Then Pyrazolone-containing anti-glyoximehydrazone ligands (H_2L^1 and H_2L^2) bearing vic-dioxime, hydrazone, and pyrazole moieties were synthesized by means of the reaction of anti-glyoximehydrazine, (GH_2), with phenylamine derivatives, and finally the metal complexes of these ligands.

All these compounds are compounds that we have previously synthesized and characterized [15,16].

3.1. Molecular docking

Molecular docking is an important method for elucidating the interactions between the synthesized compound and target protein and finding the one with the highest potential value [24]. In this study, H_2L^1, H_2L^2 ligands and their nickel(II), cobalt(II) and copper(II) metal complexes were docked with EGFR Kinase domain complexed with tak-285 (PDB ID: 3POZ) and human androgen receptor T877A mutant (PDB ID: 2OZ7) in order to evaluate the interactions occurred between the compounds and the target receptors.

Binding energy values and the interactions between the compounds and target proteins were listed in Table 1 in detail. In addition, Figs. 1–4 shows the 3D diagram, hydrogen bonding interaction and the interactions of compounds with target proteins 3POZ and 2OZ7.

Compared to H_2L^1 and H_2L^2, nickel(II), cobalt(II) and copper(II) metal complexes had higher binding energies against 3POZ and 2OZ7 target proteins (Table 1). The docking results revealed that the most promising compounds towards target receptor 3POZ were $Ni(H_2L^1)_2$ and

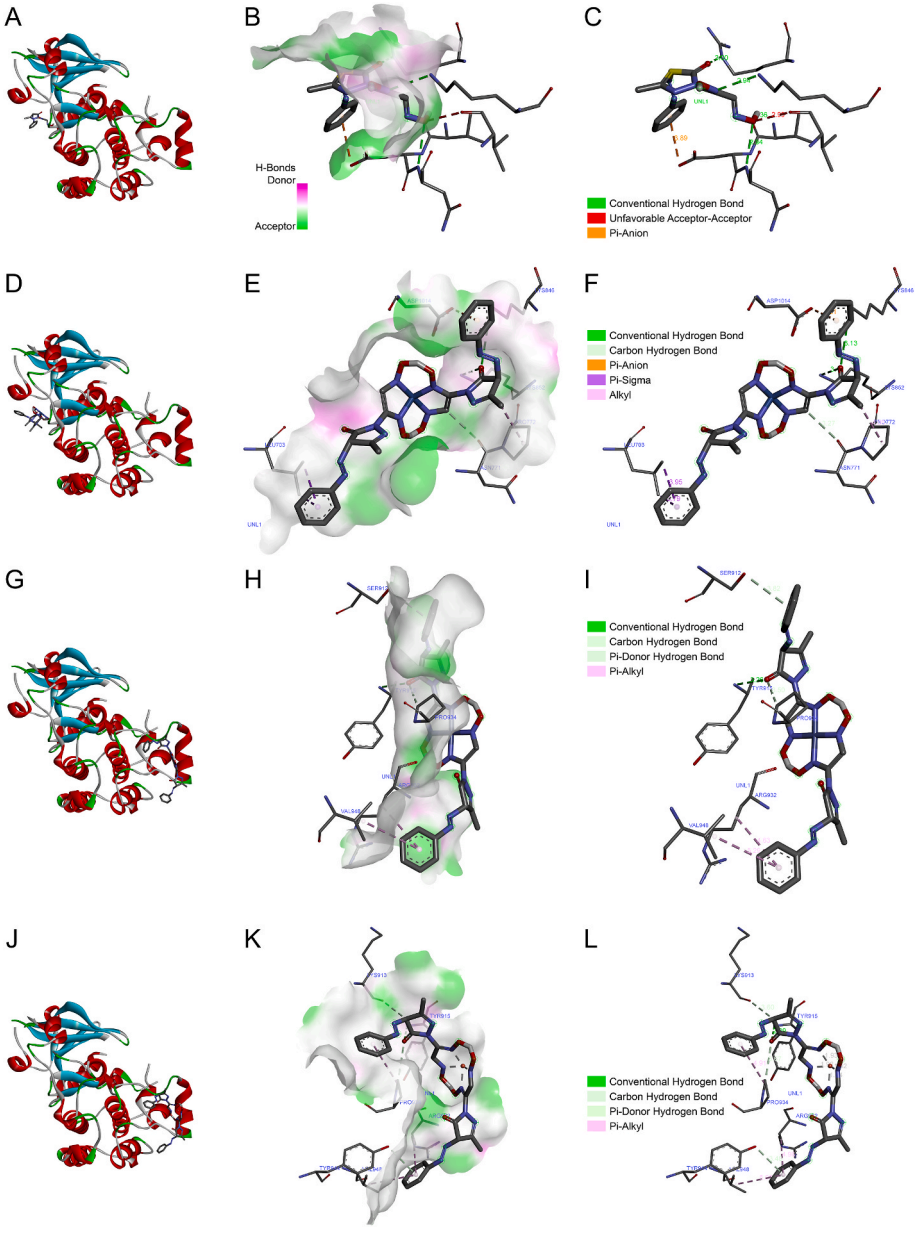

Fig. 1. A, D, G, J) 3-D positioning diagram; B, E, H, K) Hydrogen bonding interaction; C, F, I, L) Interactions of H_2L^1, $Ni(H_2L^1)_2$, $Co(H_2L^1)_2$ and $Cu(H_2L^1)_2$ with 3POZ, respectively.

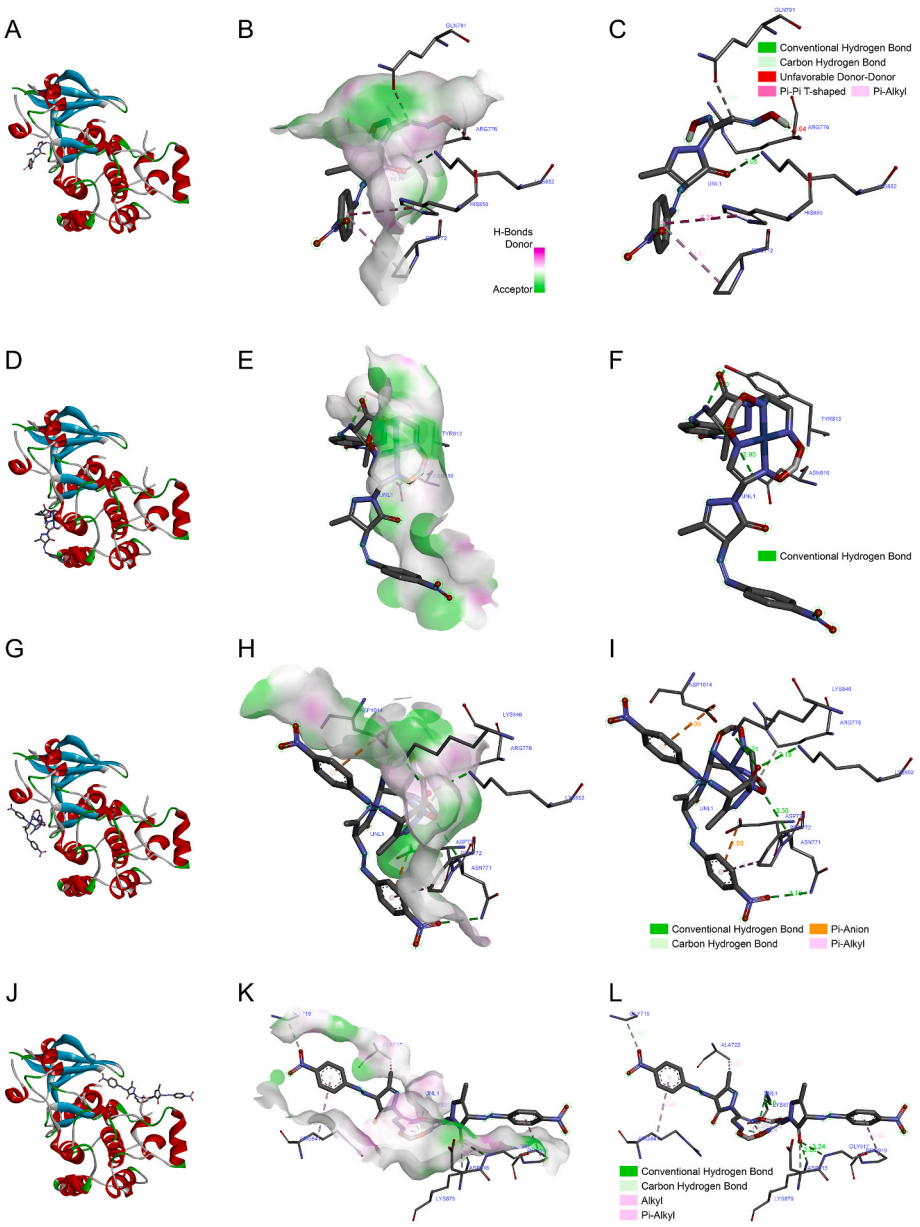

Fig. 2. A, D, G, J) 3-D positioning diagram; B, E, H, K) Hydrogen bonding interaction; C, F, I, L) Interactions of H_2L^2, $Ni(H_2L^2)_2$, $Co(H_2L^2)_2$ and $Cu(H_2L^2)_2$ with 3POZ, respectively.

$Cu(H_2L^1)_2$ which had the lowest affinity scores −9.1 kcal/mol and −9.2 kcal/mol, respectively. It was observed that H_2L^1 ligand predominantly had conventional hydrogen bonds with 3POZ and made a pi-anion interaction. $Ni(H_2L^1)_2$ complex had two conventional hydrogen bonds, one carbon-hydrogen bond, one pi-anion, two pi-sigma and one alkyl interaction. Furthermore, $Co(H_2L^1)_2$ complex had two conventional hydrogen bonds, one pi-donor hydrogen bond and two pi-alkyl for hydrophobic interactions. $Cu(H_2L^1)_2$ which had the higher affinity towards 3POZ had one conventional hydrogen bond, two carbon-hydrogen bonds, one pi-donor hydrogen bond and three hydrophobic pi-alkyl interactions with various amino acids of 3POZ (Table 1). Also, H_2L^2 was bound to 3POZ through only two conventional hydrogen bonds. $Ni(H_2L^2)_2$ and $Co(H_2L^2)_2$ had fewer interactions with 3POZ such that they had only two and three conventional hydrogen bonds, respectively. However, $Cu(H_2L^2)_2$ which had the highest binding energy (−8.5 kcal/mol) towards 3POZ when compared to H_2L^2 and its other metal complexes had three conventional hydrogen bonds, two carbon-hydrogen bonds, one alkyl and two pi-alkyl interactions.

The molecular docking with 2OZ7 target receptor revealed that H_2L^1 and H_2L^2 had the lowest binding energy values of −5.8 kcal/mol and −6.4 kcal/mol, respectively. Among H_2L^1 ligand's metal complexes the most potent one was determined as $Co(H_2L^1)_2$ with a binding energy value of −8.9 kcal/mol. According to Table 1, H_2L^1 had two conventional hydrogen bonds, and predominantly had hydrophobic interactions like pi-sigma, alkyl and pi-alkyl with various amino acids of 2OZ7 target receptor. $Ni(H_2L^1)_2$ complex had one pi-pi t-shaped, two alkyl and four pi-alkyl interactions, $Co(H_2L^1)_2$ complex had three conventional hydrogen bonds, two pi-pi stacked and two pi-alkyl interactions and $Cu(H_2L^1)_2$ had three conventional and one pi-donor hydrogen bonds, also, hydrophobic interactions like pi-pi t-shaped, alkyl and pi-alkyl with the amino acids. Furthermore, H_2L^2 bounded to 2OZ7 target receptor through one pi-cation, one alkyl and two pi-alkyl interactions. $Ni(H_2L^2)_2$ had the lowest binding energy value (−7.8 kcal/mol) among all the metal complexes and had four conventional hydrogen and two carbon-hydrogen bonds and one pi-pi stacked interaction with the amino acids of 2OZ7. $Co(H_2L^2)_2$ and $Cu(H_2L^2)_2$ complexes were observed to have the highest affinities to 2OZ7 which had binding energy values of −9.0 kcal/mol and −9.4 kcal/mol,

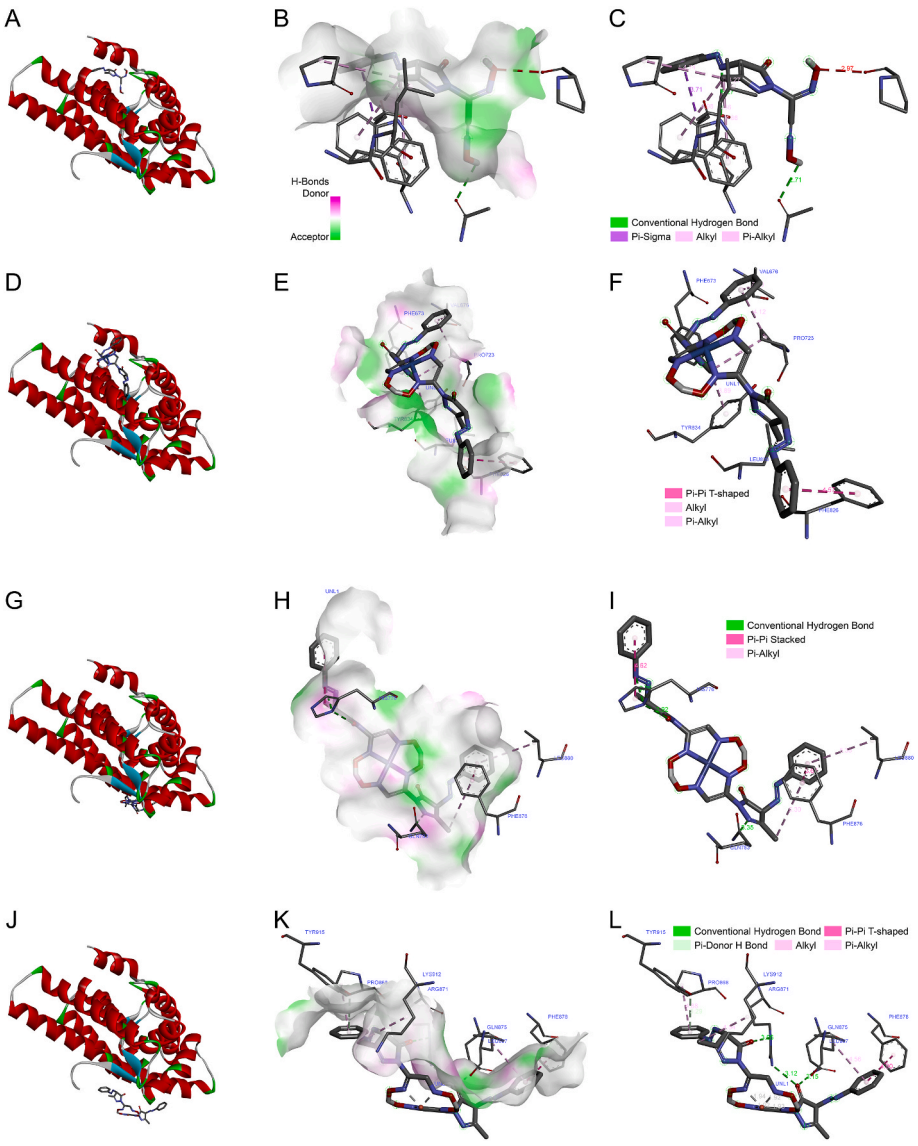

Fig. 3. A, D, G, J) 3-D positioning diagram; B, E, H, K) Hydrogen bonding interaction; C, F, I, L) Interactions of H_2L^1, $Ni(H_2L^1)_2$, $Co(H_2L^1)_2$ and $Cu(H_2L^1)_2$ with 2OZ7, respectively.

respectively. $Co(H_2L^2)_2$ had three conventional hydrogen bonds, one electrostatic interaction pi-anion, one pi-sigma and one pi-pi stacked interaction. In addition, $Cu(H_2L^2)_2$ is bounded with four conventional hydrogen bonds, one carbon-hydrogen bond, three alkyl and two pi-alkyl interactions to 2OZ7 target receptor protein.

In the manner of validation of the molecular docking method, the most stable conformations of the tak-285 (PDB ID:03P) ligand in EGFR Kinase domain complexed with tak-285 and cyproterone acetate (PDB ID:CA4) ligand in human androgen receptor T877A mutant were predicted by self –docking. Superimposed views of the co-cristalized ligand and re-docked ligands of EGFR Kinase domain complexed with tak-285 and human androgen receptor T877A mutant were presented in Fig. 5 and their RMSD values were 0.741 and 1.015, respectively.

3.2. Geometrical optimization

The optimization of the compounds were performed by using hybrid correlation functional (B3LYP) in conjunction with the basis sets 6–311 (d, p) [25–27]. The optimized structures of the compounds were depicted in Fig. 6.

3.3. Quantum chemical calculations

Molecular orbital calculation results were presented in Table 2. According to the results obtained, $Co(H_2L^2)_2$ had the smallest and H_2L^1 ligand had the biggest ΔE_{gap} values of 0.055 eV and 0.157 eV, respectively. Since the ΔE_{gap} value of H_2L^1 was found to be the highest, it would need more energy to jump from HOMO to LUMO excited state [28]. $Co(H_2L^2)_2$ had the lowest η value and the highest σ value which were associated with the lowest ΔE_{gap} value and made it the most reactive one. Furthermore, $Co(H_2L^2)_2$ had the highest ω which was related to a potent higher electrophilic character among the others.

HOMO and LUMO plots of H_2L^1 and its metal complexes were depicted in Fig. 7. More electron density localization was shown over the Pyrazolone ring and side chain, however slightly localized over the phenyl ring in HOMO contour of H_2L^1 and in LUMO contour it was densed over the phenyl ring (Fig. 7A). For HOMO contours of nickel(II), cobalt(II) and copper(II) complexes of H_2L^1 the electron density localized over the square planar metal complex area (Fig. 7B, C, D). However, for LUMO contour of $Cu(H_2L^1)_2$ the electron density distribution covered the molecule, for Ni $(H_2L^1)_2$ it was localized over the square planar metal complex area and for $Co(H_2L^1)_2$ the localization was

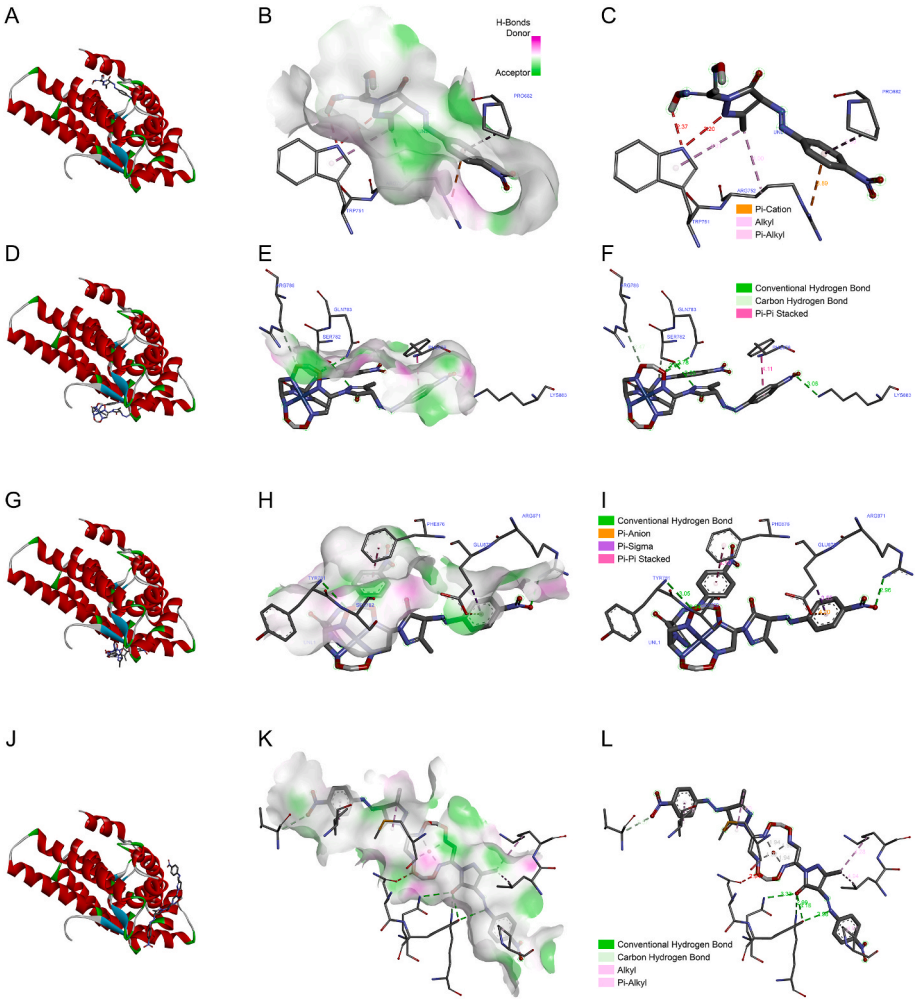

Fig. 4. A, D, G, J) 3-D positioning diagram; B, E, H, K) Hydrogen bonding interaction; C, F, I, L) Interactions of H_2L^2, $Ni(H_2L^2)_2$, $Co(H_2L^2)_2$ and $Cu(H_2L^2)_2$ with 2OZ7, respectively.

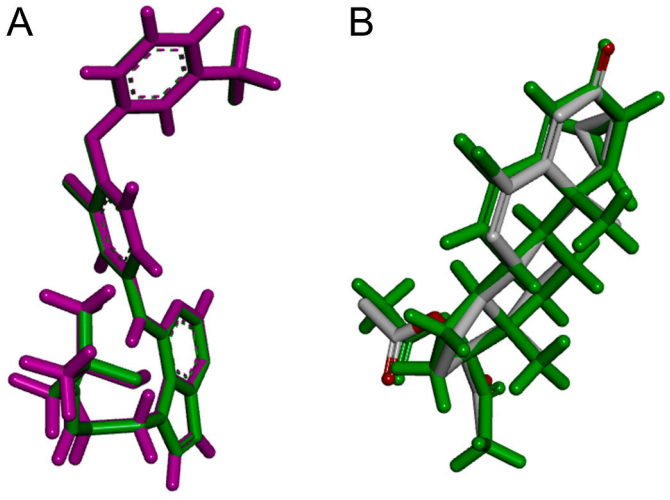

Fig. 5. Self-docking poses of A) 3POZ and B) 2OZ7 with RMSD values of 0.741 and 1.015, respectively.

intensely over one phenyl ring and the square planar metal complex (Fig. 7B, C, D). Similar to the contours of H_2L^1 for H_2L^2 ligand's HOMO contour, the localization of electron density was observed to be intense over the Pyrazolone ring and side chain, not over the phenyl ring (Fig. 8A). For metal complexes of H_2L^2 the electron density condensed over the square planar metal complex area (Fig. 8B, C, D). Furthermore, the electron density is distributed intensely over the phenyl ring for H_2L^2 LUMO contour (Fig. 8A). For $Ni(H_2L^2)_2$, $Co(H_2L^2)_2$ and $Cu(H_2L^2)_2$ the electron density localized over only one phenyl ring (Fig. 8B, C, D).

3.4. ADMET results

In drug discovery, the compounds were expected to have bioactivity parameters in the recommended range. The compounds that have a bioactivity score higher than zero are highly bioactive, which were between −5.0 – 0 are moderately active and smaller than −5.0 are inactive [29]. In this study, the bioactivity scores of the ligands and their metal complexes were determined by subjecting them to calculations performed by Molinspiration web-based tool. The results were predicted in Table 3. The values for the compounds obtained in our study range from −1.68 to 0.12, which means that our compounds have moderate bioactivity. Accordingly, with some modifications to their chemical structure, they can be expected to act as potential drugs [30].

4. Conclusion

In this work, ligands (H_2L^1 and H_2L^2) bearing vic-dioxime, hydrazone, and pyrazole moieties were synthesized from the reaction of antiglyoximehydrazine, (GH_2), with phenylamine derivatives and their nickel(II), cobalt(II) and copper(II) complexes were obtained and

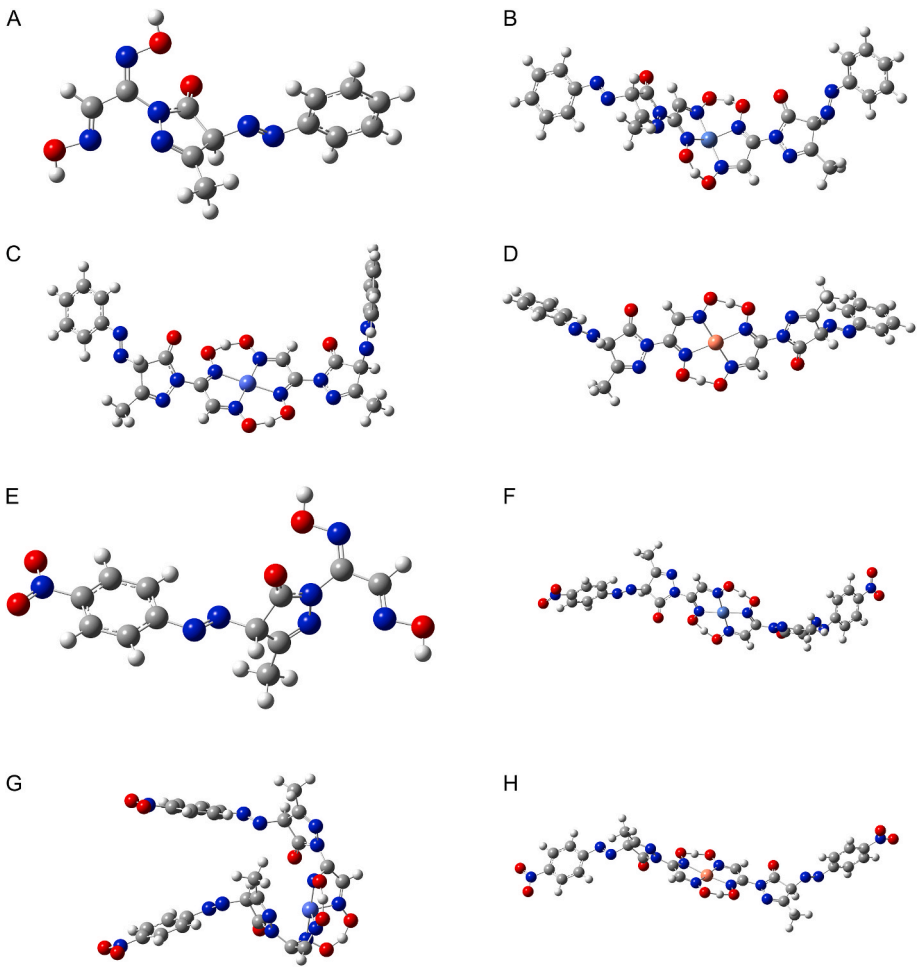

Fig. 6. Optimized structures of A) H_2L^1, B) $Ni(H_2L^1)_2$, C) $Co(H_2L^1)_2$, D) $Cu(H_2L^1)_2$, E) H_2L^2, F) $Ni(H_2L^2)_2$, G) $Co(H_2L^2)_2$ and H) $Cu(H_2L^2)_2$ respectively.

Table 2
HOMO-LUMO energy values and quantum chemical calculation results.

Compound	E_{HOMO} (eV)	E_{LUMO} (eV)	ΔE_{gap} (eV)	χ	π	η	σ	ω
H_2L^1	−0.249	−0.092	0.157	0.171	−0.171	0.079	12.739	0.185
$Ni(H_2L^1)_2$	−0.216	−0.111	0.105	0.164	−0.164	0.053	19.048	0.255
$Co(H_2L^1)_2$	−0.214	−0.103	0.111	0.159	−0.159	0.056	18.018	0.226
$Cu(H_2L^1)_2$	−0.208	−0.103	0.105	0.156	−0.156	0.053	19.048	0.230
H_2L^2	−0.260	−0.129	0.131	0.195	−0.195	0.066	15.267	0.289
$Ni(H_2L^2)_2$	−0.238	−0.135	0.103	0.187	−0.187	0.052	19.417	0.338
$Co(H_2L^2)_2$	−0.226	−0.171	0.055	0.199	−0.199	0.028	36.364	0.716
$Cu(H_2L^2)_2$	−0.223	−0.137	0.086	0.180	−0.180	0.043	23.256	0.377

evaluated, according to the literature [15–17]. For investigating the possible interactions between the compounds and target protein receptors molecular docking was performed. Metal complexes had higher binding affinities against target proteins 3POZ and 2OZ7. The most promising compounds for 3POZ were $Ni(H_2L^1)_2$ and $Cu(H_2L^1)_2$. However, for the 2OZ7 target receptor, $Co(H_2L^2)_2$ and $Cu(H_2L^2)_2$ were the possible hit compounds. Furthermore, $Co(H_2L^2)_2$ was found to be the most reactive one among others due to its highest value of η and the lowest value of ΔE_{gap}. Moreover, $Co(H_2L^2)_2$ had the highest ω which was related to a potent higher electrophilic character among the others. It was determined that all the compounds had moderate bioactivity.

In conclusion, compounds need to be tested with further chemical modifications to obtain new and effective anticancer molecules. These nickel(II), cobalt(II), and copper(II) complexes could be powerful hit compounds for anti-cancer drug discovery studies.

Funding

This research did not receive any specific grant from funding agencies in the public, commercial, or not-for-profit sectors.

Declaration of competing interest

The authors declare that they have no known competing financial interests or personal relationships that could have appeared to influence the work reported in this paper.

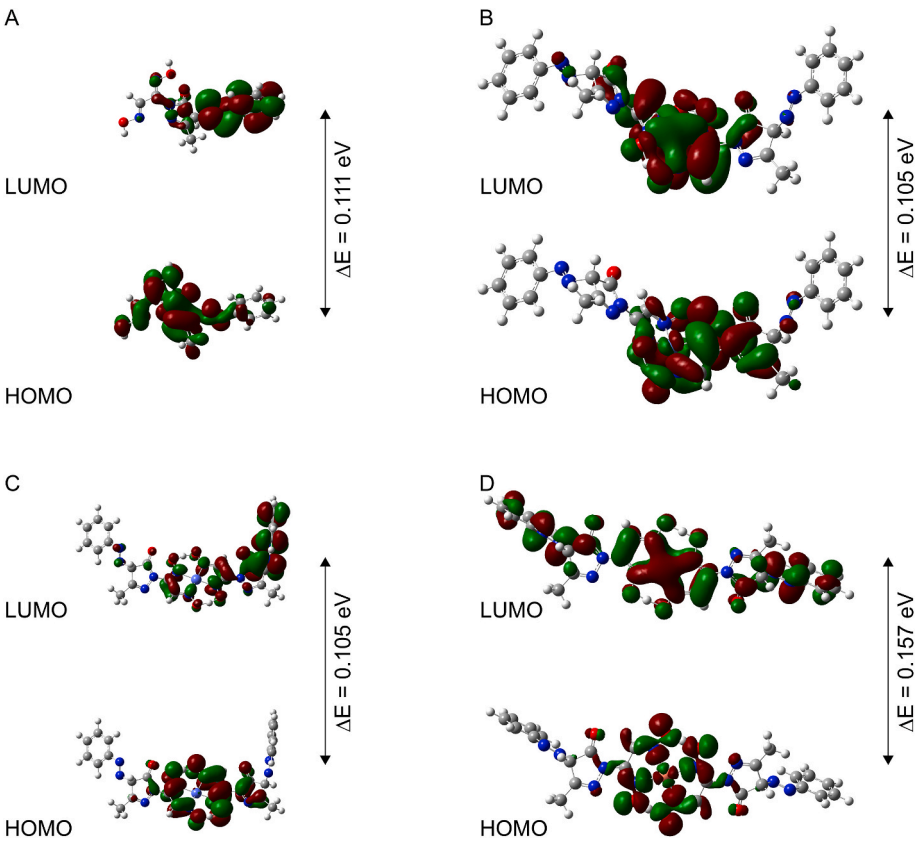

Fig. 7. The FMO contour diagrams of A) H_2L^1, B) $Ni(H_2L^1)_2$, C) $Co(H_2L^1)_2$, D) $Cu(H_2L^1)_2$, respectively.

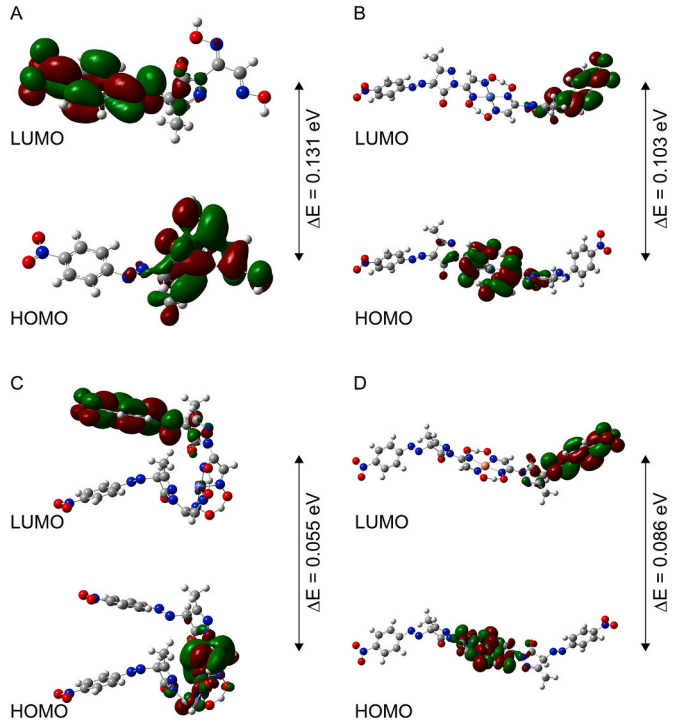

Fig. 8. The FMO contour diagrams of A) H_2L^2, B) $Ni(H_2L^2)_2$, C) $Co(H_2L^2)_2$, D) $Cu(H_2L^2)_2$, respectively.

Table 3
The bioactivity scores of H_2L^1, H_2L^2 and their metal complexes.

Compound	GPCRL	ICM	KI	NRL	PI	EI
H_2L^1	−0.42	−0.51	−0.34	−0.95	−0.47	−0.12
$Ni(H_2L^1)_2$	−0.32	−0.88	−0.40	−0.84	−0.24	−0.54
$Co(H_2L^1)_2$	−0.32	−0.88	−0.40	−0.84	−0.24	−0.54
$Cu(H_2L^1)_2$	−0.32	−0.88	−0.40	−0.84	−0.24	−0.54
H_2L^2	−0.48	−0.50	−0.42	−0.87	−0.48	−0.21
$Ni(H_2L^2)_2$	−0.97	−1.68	−1.28	−1.68	−0.69	−1.30
$Co(H_2L^2)_2$	−0.97	−1.81	−1.28	−1.68	−0.69	−1.30
$Cu(H_2L^2)_2$	−0.97	−1.81	−1.28	−1.68	−0.69	−1.30

References

[1] B. Kirste, Applications of density functional theory to theoretical organic chemistry, Chem. Sci. J. 7 (2016) 2.
[2] M. Toy, H. Tanak, H. Şenöz, Experimental and DFT computational studies of novel 3-(pcyanophenyl)-5-(o,m,p-nitrophenyl)-5-phenylformazans, J. Mol. Struct. 1213 (2020), 128178.
[3] M. Cheng, B. De, N.G. Almstead, S. Pikul, M.E. Dowty, C.R. Dietsch, C.M. Dunaway, F. Gu, L.C. Hsieh, M.J. Janusz, Y.O. Taiwo, M.G. Natchus, T. Hudlicky, M. Mandel, Design, synthesis, and biological evaluation of matrix metalloproteinase inhibitors derived from a modified proline scaffold, J. Med. Chem. 42 (1999) 5426–5436, https://doi.org/10.1021/jm9904699.
[4] N. Kitajima, Y. Moro-oka, Copper-dioxygen complexes. Inorganic and bioinorganic perspectives, Chem. Rev. 94 (1994) 737.
[5] D.E. Fenton, Biocoordination Chemistry, Oxford University Press, Oxford, 1997.
[6] S. Kuse, S. Motomizu, K. Tôei, o-Diketonedioxime compounds as analytical reagents for the spectrophotometric determination of nickel, Anal. Chim. Acta 70 (1974) 65.
[7] X.H. Liu, P. Cui, B.A. Song, P.S. Bhadury, H.L. Zhu, S.F. Wang, Synthesis, structure and antibacterial activity of novel 1-(5-substituted-3-substituted-4,5-dihydropyrazol-1-yl) ethanone oxime ester derivatives, Bioorg. Med. Chem. 16 (2008) 4075–4082.
[8] G. Ouyang, Z. Chen, X.J. Cai, B.A. Song, P.S. Bhadury, S. Yang, L.H. Jin, W. Xue, D. Y. Hu, S. Zeng, Synthesis and antiviral activity of novel pyrazole derivatives containing oxime esters group Bioorg, Med. Chem. 16 (2008) 9699–9707.
[9] I.M. Abbas, M.A. Abdallah, S.M. Gomha, M.S.H. Kazem, Synthesis and antimicrobial activity of novel azolopyrimidines and pyrido-triazolo-pyrimidinones incorporating pyrazole moiety, J. Heterocycl. Chem. 54 (2017) 3447–3457.
[10] M.A. Abdalla, S.M. Gomha, M.R. Abdelaziz, N. Serag, Synthesis and antiviral evaluation of some novel thiazoles and 1,3-thiazines substituted with pyrazole moiety against rabies virus, Turk. J. Chem. 40 (2016) 441–453.
[11] M. Anzaldi, C. Maccio, M. Mazzei, M. Bertolotto, L. Ottonello, F. Dallegri, A. Balbi, Antiproliferative and proapoptotic activities of a new class of pyrazole derivatives in HL-60 cells, Chem. Biodivers. 6 (2009) 1674–1687.
[12] A. El-Shafei, A.A. Fadda, A.M. Khalil, T.A.E. Ameen, F.A. Badria, Synthesis, antitumor evaluation, molecular modeling and quantitative structure-activity relationship (QSAR) of some novel arylazopyrazolodiazine and triazine analogs, Bioorg. Med. Chem. 17 (2009) 5096–5105.
[13] I. Althagafi, N.M. El-Metwaly, M.G. Elghalban, T.A. Farghaly, M.A. Khedr, Synthesis of pyrazolone derivatives and their nanometer Ag(I) complexes and physicochemical, DNA binding, antitumor, and theoretical implementations, Bioinorgan. Chem. Appl. 2018 (2018), 2727619.
[14] M.A. Alhasani, T.A. Farghaly, H.A. El-Ghamry, Mono- and bimetallic complexes of pyrazolone based ligand: synthesis, characterization, antitumor and molecular docking studies, J. Mol. Struct. 1249 (2022), 131607.
[15] N. Sarikavakli, G. İrez, Synthesis and complex formation of some novel vicDioxime derivatives of hydrazones, Turk. J. Chem. 29 (2005) 107–116.
[16] N. Sarikavakli, E. Koç, M.H. Meshari Aljohani, S.K. Mustafa, Synthesis, spectral analysis and biological potency of hydrazoneoxime ligands incorporating pyrazolone moiety and their metal complexes, orient, J. Chem. 36 (2020) 119.
[17] F. Erol, Synthesis, characterization, absorption and fastness properties of novel monoazo dyes derived from 1-Phenyl-3-amino-4-(2-thiazolilazo)pyrazol-5-one, J. Braz. Chem. Soc. 31 (2020) 1815.
[18] O. Trott, A.J. Olson, AutoDock Vina, Improving the speed and accuracy of docking with a new scoring function, efficient optimization, and multithreading, J. Comput. Chem. 31 (2009) 455–461.
[19] K. Onodera, K. Satou, H. Hirota, Evaluations of molecular docking programs for virtual screening, J. Chem. Inf. Model. 47 (2007) 1609–1618.
[20] A.T. Onawole, T.U. Kolapo, K.O. Sulaiman, R.O. Adegoke, Structure based virtual screening of the Ebola virus trimeric glycoprotein using consensus scoring, Comput. Biol. Chem. 72 (2018) 170–180.
[21] M.J. Frisch, et al., Gaussian 09, Revision A.02, Gaussian, Inc., Wallingford, CT, 2009.
[22] K.O. Sulaiman, T.U. Kolapo, A.T. Onawole, M.A. Islam, R.O. Adegoke, S. O. Badmus, Molecular dynamics and combined docking studies for the identification of Zaire ebola virus inhibitors, J. Biomol. Struct. Dyn. 37 (12) (2019) 3029–3040.
[23] www.molinspiration.com.
[24] E. Başaran, R. Çakmak, S. Akkoç, S. Kaya, Combined experimental and theoretical analyses on design, synthesis, characterization, and in vitro cytotoxic activity evaluation of some novel imino derivatives containing pyrazolone ring, J. Mol. Struct. 1265 (2022), 133427.
[25] A.D. Becke, Density-functional thermochemistry. III. The role of exact exchange, J. Chem. Phys. 98 (1993) 5648–5651, https://doi.org/10.1063/1.464913.
[26] C. Lee, W. Yang, R.G. Parr, Development of the Colle-Salvetti correlation-energy formula into a functional of the electron density, Phys. Rev. B 37 (1988) 785–789, https://doi.org/10.1103/PhysRevB.37.785.
[27] B. Miehlich, A. Savin, H. Stoll, H. Preuss, Results obtained with the correlation energy density functionals of becke and Lee, Yang and Parr, Chem. Phys. Lett. 157 (1989) 200–206, https://doi.org/10.1016/0009-2614(89)87234-3.
[28] J. Ferdous, S.M.A. Kawsar, Thermochemical, molecular docking and ADMET studies of some methyl α-D-glucopyranoside derivatives, Chittagong Univ. J. Biol. Sci. 42 (1) (2020) 58.
[29] A. Verna, Lead finding from phyllanthusdebelis with hepatoprotective potentials, Asian Pac. J. Trop. Biomed. 1 (2012) 735–737.
[30] T. Khan, S. Dixit, R. Ahmad, S. Raza, I. Azad, S. Joshi, A.R. Khan, Molecular docking, PASS analysis, bioactivity score prediction, synthesis, characterization and biological activity evaluation of a functionalized 2-butanone thiosemicarbazone ligand and its complexes, J. Chem. Biol. 10 (3) (2017) 91–104.